Economic optimization of coastal flood defense systems

Dupuits, E. J C; Schweckendiek, T.; Kok, M.

DOI
10.1016/j.ress.2016.10.027

Publication date
2017

Document Version
Accepted author manuscript

Published in
Reliability Engineering & System Safety

Economic Optimization of Coastal Flood Defense Systems

E.J.C. Dupuits[a], T. Schweckendiek[a,b], M. Kok[a]

[a]*Delft University of Technology, Faculty of Civil Engineering and Geosciences, P.O. Box 5048, 2600 GA Delft, Netherlands*
[b]*Deltares Unit Geo-engineering, P.O. Box 177, 2600 MH Delft, Netherlands*

Abstract

Coastal flood defense systems can consist of multiple lines of defense. In case of a system with a front and a rear defense (e.g. a storm surge barrier and levees), the front defense can improve the reliability of the rear defense by reducing the load on this rear defense. This paper develops a framework in order to assess whether including the influence of such a load reduction influences the economically optimal safety targets of both defenses. The economic optimization is carried out using two approaches: a simplified method developed to explore the behavior of the economic optimization with a front and rear defense, and a numerical framework geared towards practical applications. The numerical framework provides more flexibility in defining risk, cost and damage functions, and emphasizes on the applicability and tractability of the necessary steps from an engineering perspective. Both approaches are used in a hypothetical case study in order to quantify the effect of including a load reduction on the economically optimal safety targets. The results indicate that if a front defense can create a significant risk reduction in a cost efficient manner, more efficient economically optimal safety targets can be found by including the load reduction.

Keywords: Economic optimization, cost-benefit analysis, system reliability, flood risk, flood defenses

1. Introduction

Coastal areas are often densely populated [24]. In order to protect the low-lying coastal areas against flooding, flood defenses can be constructed [14]. These flood defenses can be part of a flood defense system with multiple lines of defense. A typical example of a coastal flood defense system with multiple lines is that of a storm surge barrier closing off a large water body and levees surrounding the large water body. Such a system is shown in Figure 1, where the barrier is the front defense and the levees are the rear defenses. Examples of such coastal flood defense systems can be found in Lake IJssel and the Eastern Scheldt in the Netherlands, and in Neva Bay, close to Saint Petersburg in Russia.

Figure 1: Simplified cross section of a front defense (B) and rear defense (A).

The front defense in Figure 1 affects the hydrodynamic conditions at the rear defense, for example by reducing surge levels. Reduced surge levels result in a reduced load at the rear defense, which means the flood risk is reduced as well. A different flood risk implies that an economic optimization will be affected as well, because in an economic optimization the sum of investment and risk costs is minimized in order to obtain economically optimal safety targets for the flood defenses (see also Sections 3 & 4). As the load reduction influences the risk cost, including this in an economic optimization can possibly lead to a different set of economically optimal safety values for both the front and rear defenses. On the other hand, not including the interaction between the two defenses simplifies the economic optimization, because the front and rear defense can then be evaluated independently from each other. For (a) analyzing the flood risk and (b) establishing economically optimal safety targets it is, hence, important to model the system appropriately, accounting for the load reduction when necessary.

Economic optimization is often done as a part of an economic cost-benefit analysis, where the risk costs use potential economic damages. Aside from economic damages, life safety is an equally important concept to consider (e.g. see [11] & [12]), and can also be used as a metric for acceptable safety targets for flood defenses. The aforementioned load reduction impacts risk, which means it can also impact a life safety analysis. However, even though there are some similarities between a life safety analysis and an economic cost-benefit analysis, a life safety analysis is a different kind of analysis. For the purpose of this paper, we therefore only focus on an economic cost-benefit analysis.

The economic optimization of a single line flood defense system has been discussed by a number of authors over the years; an example of a recent application can be found in [19]. Already in 1956, Van Dantzig described the economic optimization of a homogeneous dike ring [30]. This case and the work by Van Dantzig has been revisited and extended by a number of authors, for example in [10] with the addition of economic growth, or in [32] where the impact of uncertainty is discussed.

The fundamental method behind these economic optimizations of single line flood defense systems has also been extended to flood defense systems with multiple lines or elements

of defense. For example, [33] described optimizing elements in a dike ring, while a polder terminal case was described in [18]. Multiple lines of defense are sometimes also referred to as 'multi-layer safety' (e.g. [1, 34, 17, 27]) or as 'hierarchical flood protection systems' [6]. In these descriptions of multiple lines of defense, the lines of defense can also include measures such as evacuation or improved spatial planning; for example, see [20] regarding optimal flood plain planning or [36] regarding optimal levee setback and height. A coastal flood defense system was analyzed in a case study by [37], but focused on the results for the Lake IJssel case in The Netherlands.

A generic description of the economically optimal safety targets of a coastal flood defense system can, for example, provide the conditions in which a front defense is needed, or how much the economically optimal safety target of a rear defense is affected by the load reduction of a front defense. To the best of our knowledge, such a generic description has not been presented yet. Therefore, the aim of this study is to develop a framework in order to assess whether including the influence of such a load reduction influences the economically optimal safety targets of a coastal flood defense system.

In order to quantify the effect of a load reduction in a coastal flood defense system (Section 2), two economic optimization approaches are proposed. The first is a simplified economic optimization method which is derived in Section 3 and is partly based on our earlier work in [8], and is used to describe the characteristics of the economically optimal safety targets of a coastal flood defense system. The second approach is a flexible numerical framework which removes a number of the limitations of the simplified method, making it more suitable for real world applications. This numerical framework, described in Section 4, combines the existing economic optimization method as used in [37], and couples it with a risk framework which is inspired by system flood risk frameworks such as described in [5]. Emphasis is placed on the applicability and tractability from an engineering perspective.

Finally, the Galveston Bay near Houston is considered as a hypothetical case study in Section 5. The Galveston Bay area has millions of inhabitants and represents a large economic value. It does not yet have an integral flood defense system, but the feasibility of such a system is being investigated because it is situated in a hurricane prone area (e.g. see [2]). Even though this study describes an economic optimization of a coastal flood defense system with a front and rear defense, the numerical framework is flexible enough to be generically applied to flood defense systems with two lines of defense. With modifications to the used risk method and optimization algorithm, the numerical framework can also be used for more than two lines of defense.

2. Flood Risk of Coastal Systems

In coastal systems, as shown in Figure 1 a front defense will reduce the load on a rear defense; thereby improving the reliability of the rear defense. In the following, this reliability improvement is first described from a physical point of view (Section 2.1). This explanation is then used to incorporate the reliability improvement in a set of risk equations (Section 2.2). Furthermore, in the remainder of this paper the term 'coastal systems' is used for coastal flood protection systems with a front and rear defense.

2.1. Load reduction by a front defense

A functioning front defense blocks partly, or even completely, the inflow into the large body of water behind the front defense. Examples of such front defenses are dams or storm surge barriers (see also Section 1). In this study, we see this inflow blockage as the primary source of load reduction. However, the effects of this load reduction depend on the properties of the basin containing the large body of water. In the following, this reduction is described from a physical stance for a subset of coastal flood defense systems that fit the description of a short basin where the 'pumping mode' assumption is valid (length of the basin $\ll$ tidal wave length).

A front defense is typically built near the inlet of a basin, denoted by width W in Figure 2. The extra inflow entering the basin during a storm event depends on the amount of blockage by the front defense. Typically, less inflow will be able to enter the basin as the front defense height increases. This is illustrated in Figure 3.

The inflow due to the storm event will result in increased basin water levels inside the basin, where the amount of basin water level increase depends on the basin surface area (S in Figure 2). However, as strong winds usually occur during

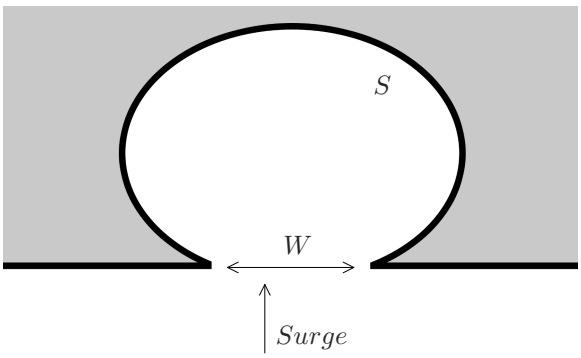

Figure 2: Top view of a typical basin, with inlet width W and surface area S.

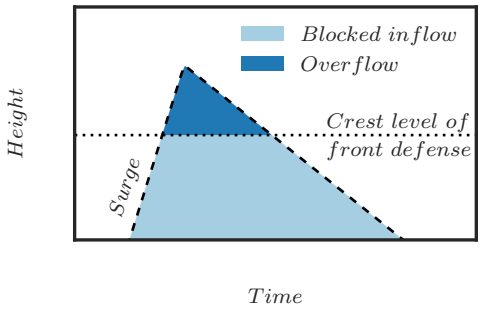

Figure 3: A front defense can block surge from flowing into a basin; however, any overflow will still enter the basin.

storm events, wind setup will at least partially negate the reduction of basin water levels, as wind setup is inversely related to basin water level (e.g. see [4]); this is particularly noticeable in shallow basins. At some point, any further increase of the front defense height will no longer result in a (significant) decrease of the basin water level. Either the front defense already completely blocks the surge inflow, or the inflow reduction is negated by an increased wind setup. In other words, at some point the load reduction by the front defense will be constant, which in the remainder of this paper will be referred to as the 'maximum load reduction'.

2.2. Annual system risk

Based on [35], we define system failure as the situation where at least one of the flood defenses has failed. Furthermore, risk is defined as the probability of failure times the damage due to failure. The annual system risk (C_R, \$/year) of a coastal flood defense system can then be described as a summation of the annual risk per flood defense:

$$C_R = P_A D_A + P_B D_B \tag{1}$$

$$P_A = P_B P_{A|B} + P_{\overline{B}} P_{A|\overline{B}} \tag{2}$$

where P_B is the failure probability of the front defense, and $P_{\overline{B}}$ is the complement of P_B. The failure probability of the rear defense, P_A, is found using the chain rule for probability and the law of total probability. Furthermore, the conditional failure probabilities of the rear defense, dependent on the failure (P_B) or functioning of the front defense ($P_{\overline{B}}$), are $P_{A|B}$ and $P_{A|\overline{B}}$, respectively. Finally, D_A and D_B (both in \$) are the damages that belong to the failure of the rear and front defense, respectively, and are assumed to be otherwise independent of the performance of the defenses (i.e. the expected damage if both A and B fail is $D_A + D_B$).

3. Simplified Economic Optimization

3.1. General

The purpose of a simplified economic optimization is to explore the behavior of the economically optimal safety levels of a coastal flood defense system with a front and rear defense. The simplifications are made both in the system description (i.e. Figure 1), and in the economic optimization assumptions (Section 3.1). The economic optimum is defined as the minimum of the total costs, similar to, for example, [30, 10]:

$$\min \left\{ TC = \sum PV\left(C_R\right) + \sum PV\left(C_I\right) \right\} \tag{3}$$

where TC is the total cost, $\sum PV\left(C_R\right)$ is the summed present value of the risk costs and $\sum PV\left(C_I\right)$ is the summed present value of the investment costs; both the risk and investment costs are defined in Section 3.2. Using the total cost equation, further equations for the economically optimal safety targets for both the front and rear defense are found in Section 3.3. Finally, the effect of including the load reduction by a front defense is discussed in Section 3.4.

For this section, the flood damages in Eq. 1 are solely based on economic valuations of damages. In a complete risk evaluation, concepts such as individual risk and societal risk should be included (e.g. see [13]). An overview of risk acceptance measures can be found in, for example, [14]. Furthermore, time dependent processes such as sea level rise or economic growth are ignored in this section. Ignoring these processes means, for the economic optimization, that only a single investment needs to be calculated. This investment is assumed to be done immediately at the start of the strengthening project; these assumptions reduce the investment term of Eq. 3 to C_I, because there is only a single term which does not need to be discounted. Including time dependent processes (e.g. see [10]) necessitates repeated investments over time, and are an integral part of the numerical economic optimization in Section 4.

3.2. Risk and investment costs

Discounting the annual risk of Eq. 1 with a real interest rate (r, > 0) over an infinite time horizon is a geometric sequence (e.g. [30]), which converges as follows:

$$\sum_{t=0}^{\infty} PV\left(C_R\right) = P_A \frac{D_A}{r} + P_B \frac{D_B}{r} \tag{4}$$

where $PV\left(C_R\right)$ is the present value of the risk cost of a system with a front and rear defense.

The investment cost relations are chosen similarly to for example [30] & [34], assuming linear functions dependent on the crest level of the defense. Because the investment is chosen to be done immediately at the start of the strengthening project, the related costs do not need to be discounted:

$$C_{I,i} = C_{f,i} + C_{v,i} h_i \tag{5}$$

where $C_{I,i}$ is the investment cost for flood defense i (which is either A or B). Furthermore, $C_{f,i}$ and $C_{v,i}$ (both > 0) are respectively the fixed and variable cost to strengthen flood defense i to height h_i. Linear investment functions are a simple way of depicting the investment costs; other types of investment functions are treated in Section 4.

3.3. Economically optimal failure probabilities

The economic optimum was defined earlier as the minimum of the total costs. The optimal values, corresponding to the location of the minimum of the total costs, can be found with the partial derivatives of the total cost equation. However, the failure probabilities have not been defined yet. We assume that a failure probability is dependent on the height h of a flood defense, and use a probability distribution dependent on this flood defense height to get to the associated annual failure probability P. For this simplified economic optimization, the annual failure probabilities of the flood defenses are simplified from annual probability of exceedance of safety level to annual exceedance of crest level h, making the assumption that overflow/overtopping is the dominant failure mechanism (analogue to [30, 10, 34]). Furthermore, we assume the annual extreme

water level to follow an exponential distribution with parameters $\alpha \geq 0$ and $\beta > 0$; other failure mechanisms besides overflow/overtopping and other distribution types are discussed in Section 4:

$$P = 1 - F(h) = \exp\left(-\frac{h-\alpha}{\beta}\right) \tag{6}$$

where h is the height of either the front defense (h_B) or the rear defense (h_A). The parameters α and β differ between the front and rear defense. For the rear defense, as the load on the rear defense is influenced by the front defense, the parameters for the rear defense can also differ depending on the state (failure/non-failure) and safety level of the front defense. The optimal values of the front and rear defense height can now be found by taking the partial derivatives of the total cost with respect to h_A and h_B, and equating these to zero (i.e. $\frac{\partial TC}{\partial h_B} = 0$ in Eq 7 and $\frac{\partial TC}{\partial h_A} = 0$ in Eq 8):

$$\frac{\beta_B C_{v,B} r + \beta_B D_A \left(\widehat{P}_B \frac{\partial \widehat{P}_{A|B}}{\partial h_B} + \widehat{P}_{\overline{B}} \frac{\partial \widehat{P}_{A|\overline{B}}}{\partial h_B}\right)}{D_B + D_A \left(\widehat{P}_{A|B} - \widehat{P}_{A|\overline{B}}\right)} = \widehat{P}_B \tag{7}$$

$$\left(\widehat{P}_B \frac{\widehat{P}_{A|B}}{\beta_{A|B}} + \widehat{P}_{\overline{B}} \frac{\widehat{P}_{A|\overline{B}}}{\beta_{A|\overline{B}}}\right) = \frac{C_{v,A} r}{D_A} \tag{8}$$

where the circonflexe above a variable indicates the economically optimal value of that variable. Furthermore, Eq. 7 contains the derivatives of the conditional failure probabilities of the rear defense with respect to the height of the front defense. The expected behavior of the failure probability of the rear defense as a function of the height of the front defense can be explained using the load reduction description of Section 2.1. This load reduction indicates that a higher front defense results in lower failure probabilities of the rear defense. Sketches of the conditional failure probabilities of the rear defense are shown in Figure 4 & 5.

The derivatives of the functions in Figure 4 & 5 start out negative, but both derivatives are assumed to converge to zero as the front defense becomes higher and the point of the maximum load reduction (see Section 2.1) is achieved. If these derivatives are indeed zero, Eq. 7 can be simplified to Eq. 9:

$$\frac{\beta_B C_{v,B} r}{D_B + D_A \left(\widehat{P}_{A|B} - \widehat{P}_{A|\overline{B}}\right)} = \widehat{P}_B \tag{9}$$

Wrongfully using the simplified Eq. 9 instead of Eq. 7 will lead to an incorrect, larger economically optimal failure probability of the front defense. This also follows from the underlying assumption of Eq. 9, which assumes that the maximum constant load reduction is valid for the entire range of safety values for the front defense; this assumption overestimates the load reduction effect of a low front defense on a rear defense.

3.4. Impact of a load reduction on the optimal safety targets

If no load reduction by the front defense on the rear defense is assumed, the two defenses can be evaluated independent of each other. In for example [34], an economically optimal solution for a single flood defense was derived. This single flood defense was characterized similarly as in Section 3.3, with a linear investment relation and exponential failure probabilities. The solution as found in [34] is shown in Eq. 10, although in a different notation:

$$\widehat{P}_{i,single} = \frac{\beta_i C_{v,i} r}{D_i} \tag{10}$$

where i can either be B for the front defense, or A for the rear defense. Eqs. 7 & 8 reduce to Eq. 10 when no load reduction is used ($\widehat{P}_{A|B} = \widehat{P}_{A|\overline{B}}$, $\frac{\partial \widehat{P}_{A|B}}{\partial h_B} = \frac{\partial \widehat{P}_{A|\overline{B}}}{\partial h_B} = 0$). The following can be said regarding the influence of a load reduction, when comparing the solutions with and without load reduction:

Front defense safety level: The front defense safety level with load reduction will be equal to, or smaller than, the safety level without load reduction, because it not only needs to cover the risk of the front defense, but also a part of the risk of the rear defense. The equation with load reduction ($\widehat{P}_B$, Eq. 7) has an extra risk term in the denominator when compared to the solution without load reduction ($\widehat{P}_{B,single}$, Eq. 10). Because all elements in this extra term are positive, and because $\widehat{P}_{A|B} \geq \widehat{P}_{A|\overline{B}}$, the optimal failure probability with load reduction is equal to, or smaller than, the optimal failure probability of a single flood defense.

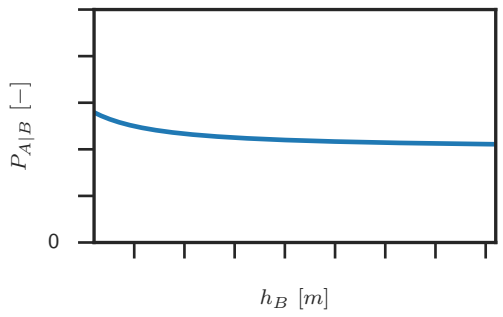

Figure 4: Even if the front defense has failed, a higher/stronger front defense (h_B) might still reduce the inflow, resulting in a lower $P_{A|B}$.

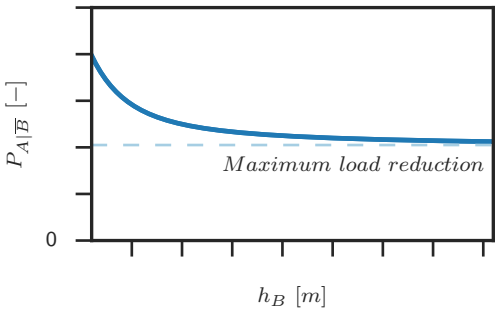

Figure 5: A higher, functioning front defense (h_B) should result in a smaller $P_{A|\overline{B}}$, but is limited by the maximum load reduction (Section 2.1).

Front defense height: Because the height and the probability of a front defense are linked via the exponential distribution of Eq. 6, this means the optimal height of the front defense with load reduction is higher than, or equal to, the height of the front defense without load reduction.

Rear defense safety level: Because of the beneficial influence of the front defense, the optimal rear defense safety level with load reduction will be equal to, or smaller than the value without load reduction. The optimal solution for the rear defense (Eq. 8) is bound between $\widehat{P}_{A|B}$ and $\widehat{P}_{A|\overline{B}}$, depending on the value of the optimal front defense safety level $\widehat{P}_B$. Assuming that $\widehat{P}_{A|B} \approx \widehat{P}_{A,single}$, this means that the optimal rear defense safety level with load reduction ($\widehat{P}_A$) is equal to, or smaller than the value without load reduction ($\widehat{P}_{A,single}$)

Rear defense height: The optimal height of the rear defense with load reduction is difficult to predict a priori: according to the exponential distribution, a smaller optimal failure probability should lead to a higher optimal height of the rear defense with load reduction. However, two different exponential distributions have been assumed for the rear defense, conditional on whether or not the front defense has failed. As the conditional failure probability with a functioning front defense ($\widehat{P}_{A|\overline{B}}$) becomes more dominant (which occurs when the front defense safety level increases), the optimal height could also go down, because the exponential distribution for a rear defense conditional on a functioning front defense leads to lower heights (since $\beta_{A|B} \geq \beta_{A|\overline{B}}$).

In order to provide a more explicit description of the behavior of the height of the rear defense, the expression for the rear defense failure probability (Eq. 2) is approximated with a single exponential distribution, which consequently also leads to a simpler expression of the optimal rear defense safety level:

$$P_A \approx e^{-\frac{h_A - \alpha_A}{\beta_X}} \tag{11}$$

$$\widehat{P}_A \approx \frac{C_{v,A} r \beta_X}{D_A} \tag{12}$$

where β_X decreases for smaller values of the front defense failure probability (P_B), and is bounded between $\beta_{A|\overline{B}}$ and $\beta_{A|B}$ (with $\beta_{A|B} \geq \beta_{A|\overline{B}}$). Combining Eqs. 11 & 12 leads to an approximate expression for $\widehat{h}_A$. If the derivative with respect to the front defense safety level (P_B) of this approximation is greater than zero, the optimal height of the rear defense ($\widehat{h}_A$) is expected to decrease for higher safety levels of the front defense (P_B):

$$\frac{\partial \widehat{h}_A}{\partial P_B} > 0 \quad \rightarrow \quad \beta_X < \exp\left(-1 - \ln\left(\frac{C_{v,A} r}{D_A}\right)\right) \tag{13}$$

Because the upper limit of β_X is $\beta_{A|B}$, it follows that the derivative will be positive, as long as the right-hand side of Eq. 13 is larger than $\beta_{A|B}$. In practice, the term $\frac{C_{v,A} r}{D_A}$ is expected to often be (much) smaller than one, which in turn leads to the right-hand side of Eq. 13 being (much) larger than one. This indicates that, in practice, a positive derivative can be expected, which means that the optimal height of the rear defenses is expected to be smaller than or equal to the optimal height without load reduction.

In conclusion, this section shows a formal reasoning why in the past flood defense systems with multiple lines of defense were built. Intuitively, building a front defense reduces the load on a rear defense, which should also reduce the required (optimal) height of a rear flood defense. The benefit of the formal treatment in this section is that, from an economic perspective, some key factors in the optimal safety targets of a coastal system were identified. Even considering the limitations imposed in this section in order to get to an analytical answer, these key factors can be used to indicate when the impact of a load reduction on the optimal safety targets is significant or not. The insight gained in this section will be applied in a (hypothetical) case study in Section 5.

4. Numerical Economic Optimization

In order to cope with more complex conditions than described hitherto, a numeric framework is proposed, shown in Figure 6. This framework describes the necessary steps to go from a system description of a coastal flood defense system, to the economic optimal safety targets of the flood defenses. The description of the framework focuses on the practical applicability and tractability of the framework and its parts from an engineering perspective. Note that the framework assumes that a flood defense type and cost function does not change over time. If, for example, an earthen levee needs to be compared with a concrete wall, multiple runs of the framework are needed. The steps in a single framework run are:

- Starting from the system description, with a predetermined system configuration of flood defenses, a system risk estimate is produced. This risk estimate is used to prescribe per flood defense the hydraulic loads, fragility functions and damage models. See also Section 4.1.

- The numerical economic optimization finds the optimal system configuration from a set of discrete safety levels for the flood defenses. Each combination of safety levels needs to have accompanying (investment) cost and flood risk values, see also Section 4.3.

- The (investment) costs are usually found using the system description and the type of flood defense, and need to be able to produce cost figures for the discrete set of safety levels. See also Section 4.2.

- Finally, the flood risk and (investment) cost values are used in a numerical economical optimization, which also uses a number of system specific input parameters such as the rate of economic growth. See also Section 4.3.

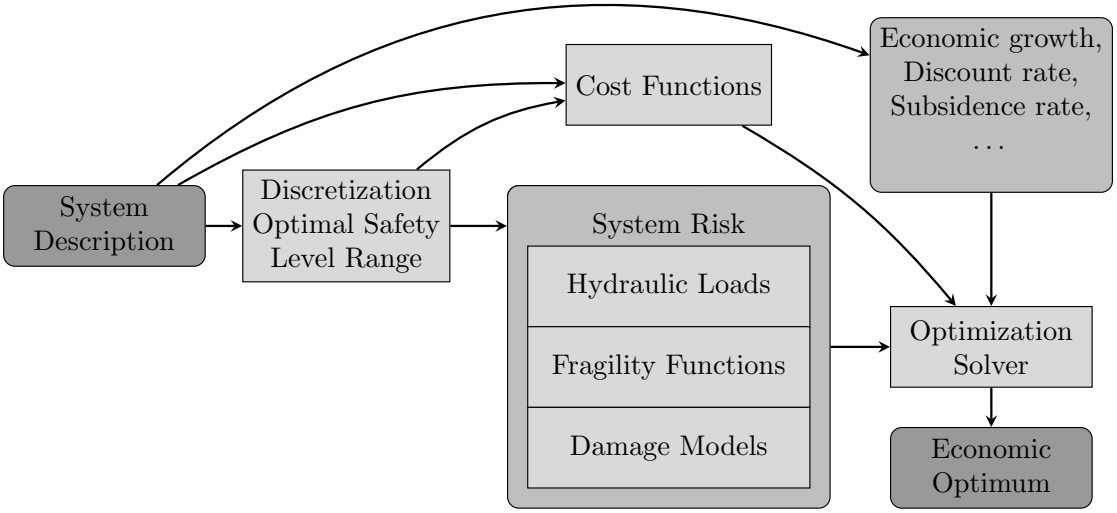

Figure 6: Overview of necessary steps in the numeric framework used to obtain economic optimal values for a coastal flood defense system.

4.1. Risk characterization

Risk is defined as probability of failure times the damage due to failure. Conceptually, the reliability of a flood defense is expressed by means of a reliability equation Z:

$$Z = Strength - Load \tag{14}$$

where failure is defined as $Z < 0$. Both the strength and (hydraulic) loads are usually considered as uncertain.

4.1.1. Hydraulic loads

Load distributions for the front defenses can be found by analyzing historical datasets, running hydrodynamic models, or a combination of the two. However, load distributions for the rear defenses can often only be found by means of hydrodynamic models, assuming the system with both a front and rear defense does not exist yet.

A common technique to acquire a distribution from an hydraulic model is Monte Carlo sampling, where a large number of model runs are made in order to approximate the load distribution. Usually a large number of samples are required, specifically for reasonable estimates of the tails. The number of required samples can be reduced by using techniques such as Importance Sampling (as applied in for example [7]).

Depending on the complexity of the hydrodynamic model and the number of required samples, approximating these load distributions can be computationally intensive. Because of this, it is recommendable to do these computations asynchronous of the economic optimization model. These computations could, for example, be stored in a table, which allows the economic optimization model to quickly look up the required values during its run; this approach is similar to what is proposed in for example [5].

4.1.2. Fragility curves

Fragility curves are a way to represent the strength term in Eq. 14 and are governed by the failure modes and type of flood defense. In the case of flood defenses, fragility curves often show the probability of failure as a function of the water level. There are multiple, possibly correlated, ways a flood defense can fail (failure mechanisms), and the water level does not necessarily need to exceed the crest height to induce failure (e.g. due to piping). In an economic optimization, typically a large number of possible flood defense designs are compared. These designs can, for example, vary the height of a flood defense. This also means that each flood defense alternative needs a fragility curve. An application of height-based fragility curves can be found in Section 5.1. For a more in-depth description on constructing fragility curves, see for example [31] or [23].

4.1.3. Damage models

Damage modelling entails combining flooding scenarios with the expected economic damage and fatalities per flooding scenario [13]. A flooding scenario is defined in [13] as "a unique sequence of events following the failure of a flood defence at one or more locations under specific high water conditions". Recognizing that in reality a large number of flooding scenarios are possible, and that these scenarios commonly use computationally intensive 2D models, two proposals were made in [13] for keeping the damage modelling tractable:

1. Define stretches of flood defenses which approximately show the same flooding pattern, independent of where the actual breach occurs in that particular stretch.
2. Find a limited set of flooding scenarios which represent the most likely scenarios.

However, the state of a flood defense will influence the most likely scenario. As an example, the most likely flooding scenario without a flood defense compared with the failure of a five meter high flood defense will likely be significantly different. A possible way of including this effect is shown in [10], where a constant ζ was introduced which depicts the "increase

of loss per cm dike heightening". A more generally applicable approach, especially for potentially widely varying safety levels, would be re-running the damage modelling for a set of representative safety levels.

4.2. Investment costs

The linear investment function of Eq. 5 in Section 3.2 is approximately valid for small increments of the height of a flood defense; this limitation was already mentioned in [30]. For earthen levees a convex function might be more suitable. This can be explained when comparing the increase of height versus the increase of the associated cross-sectional area: the relative increase in cross-sectional area will be more than the relative height increase (see also for example page 145 in [33]). A convex function is used in for example [10] or [16]. Specifically, in [16] an exponential function is used. This function is repeated here with a slightly different notation for consistency with the earlier used symbols:

$$C_{I,i} = \left(C_{f,i} + C_{v,i}u_i\right) e^{\lambda(u_i+W)}\,, \tag{15}$$

where u_i is the height increase of the flood defense, W is the sum of all the previous height increases, and λ is a scale parameter [16]. A similar equation and estimattes for $C_{f,i}$, $C_{v,i}$ and λ are shown in [9], specifically Appendix C.4. The data in [9] also showed that the estimates for $C_{f,i}$, $C_{v,i}$ and λ can differ significantly per case study. Preliminary estimates for a wider range range of flood defenses in an international context can be found in for example [15]. If λ is equal to zero, the exponential relation in Eq. 15 reduces to a linear investment relation.

4.3. Economic optimization

In a general sense, an economic optimization model indicates when to (repeatedly) invest where, and how much, by minimizing of the total costs (Eq. 3). Examples of recent numerical economic optimization methods can be found in [3] or [38]. The methods by [3, 37, 38] use similar techniques in order to quickly get from a large set of potential combinations of risk and investment costs to an optimal investment path with minimal total costs. A conceptual visualization of the set of potential combinations for the risk costs is shown in Figure 7. These techniques involve linear or nonlinear programming. A method sharing the same fundamental approach from [38] was used in [37] to find the economic optimal safety levels for the Lake IJssel case; Section 5 uses this method as well.

5. Application

This section presents an application of both the economic optimization approaches in Section 3 & 4 in order to quantify the difference of including the load reduction effect of a front defense. The application is based on the work from a real, ongoing case study in the Galveston Bay area near Houston, Texas, which has been significantly reduced in complexity. Therefore, the results should not be considered directly for decision making for the Galveston Bay area. The Galveston Bay consists of a large bay with barrier islands (Figure 8), and hosts millions

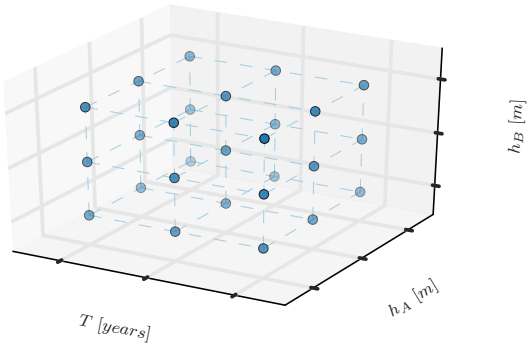

Figure 7: Conceptual illustration of the solution space of risk costs for a front (h_B) and rear defense (h_A). Each dot represents a unique combination of time T and heights, and each unique combination is coupled to a risk estimate. This risk estimate is calculated for the period which starts at the current time T and ends at the next point in time.

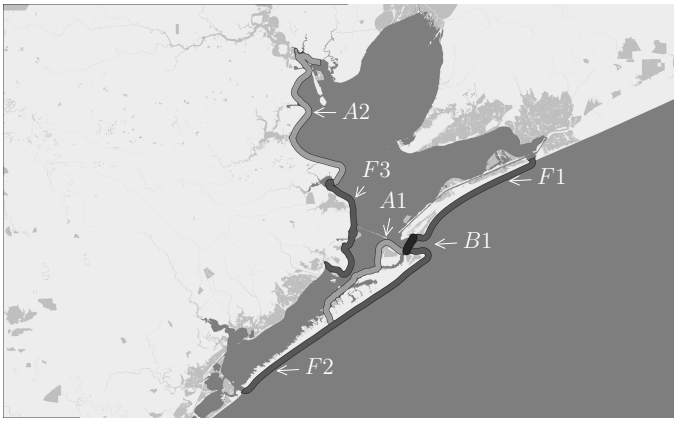

Figure 8: Galveston Bay area with contours indicating the defense types for the hypothetical application. Three types of defenses exist: A defense with a fixed safety level ($F1$, $F2$ and $F3$), a front defense ($B1$) and a rear defense ($A1$ and $A2$). Note that the contours are indicative only and do not necessarily correspond with the position of existing flood defenses. Map data is modified from OpenStreetMap (© OpenStreetMap contributors, http://www.openstreetmap.org/copyright).

of people and a large economic value. It does not yet have an integral flood defense system, but the feasibility is being investigated because the area is hurricane prone (e.g. see [2]).

For this hypothetical case study, a number of defenses has been set to a fixed level: defenses $F1$, $F2$ and $F3$ in Figure 8. Moreover, only a single system configuration will be considered: the number, type and location of all the considered flood defenses is predetermined and shown in Figure 8. Consequently, this leaves Figure 8 with only three defenses which will be part of the economic optimization: a single front defense in the form of a storm surge barrier ($B1$), and two rear defenses ($A1$ and $A2$).

5.1. Risk characterization

Four separate flood prone areas can be identified: the island protected by $F1$, the island protected by $F2$ and $A1$, and two main

land areas protected by $F3$ and $A2$. This leads to the following annual risk for the system ($C_{R,bay}$):

$$C_{R,bay} = P_{F1}D_{F1} + (P_{F2} + P_{A1})\,D_{F2} + P_{F3}D_{F3} + P_{A2}D_{A2} \quad (16)$$

where the defenses $F2$ and $A1$ are assumed to protect the same area (D_{F2}), and are assumed to be independent with a negligible probability that $F2$ and $A1$ fail simultaneously. Eq. 16 is simplified further by assuming that the defenses $B1$ and $F1$ do not protect any value of their own ($D_{B1} \approx 0$, $D_{F1} \approx 0$):

$$C_{R,bay} = (P_{F2} + P_{A1})\,D_{F2} + P_{F3}D_{F3} + P_{A2}D_{A2} \quad (17)$$

where the flood damage estimates D_{F2}, D_{F3} and D_{A2} will be loosely based on the residential and industrial flood damage estimates found in [25, Section 6]. Finally, the annual failure probabilities of the flood defenses behind the front defense $B1$ (i.e. $A1$, $A2$ and $F3$) can be elaborated in a similar way as in Section 2.2 to incorporate the possible load reduction of the front defense:

$$P_{A1} = P_{B1}P_{A1|B1} + P_{\overline{B1}}P_{A1|\overline{B1}} \quad (18)$$

$$P_{A2} = P_{B1}P_{A2|B1} + P_{\overline{B1}}P_{A2|\overline{B1}} \quad (19)$$

$$P_{F3} = P_{B1}P_{F3|B1} + P_{\overline{B1}}P_{F3|\overline{B1}} \quad (20)$$

5.1.1. Loads and resistance

The hydraulic loads used in this illustration are based on the following assumptions:

- The load distributions for defenses $A1$, $A2$ and $F3$, under influence of either a functioning or failed front defense $B1$, are modelled using a hydraulic model as proposed in [26]. This 1D hydraulic model simulates the hurricane surge and wind setup inside the bay; where a front defense can influence the surge by reducing the inflow into the bay. In case of a failed front defense, the water is assumed to flow unrestricted into the bay (i.e. as if the front defense was never built); this is a conservative assumption as in reality even a failed front defense will still restrict flow into the bay.
- All flood defenses are assumed to have a ground level of two meters above Mean Sea Level (MSL). In other words, even without any flood defense this means that flooding can only occur if the water levels exceed two meters above MSL. The only exception is the front defense $B1$, which is assumed to have a ground level at MSL. Because of limitations in the hydraulic model, a front defense height below MSL is not considered.
- The maximum, constant load reduction effect by a front defense on the water levels behind the front defense is applied for every front defense height. This reduces the number of hydraulic load computations, but overestimates the impact of a front defense, especially at small heights (see also Section 2.1);
- The defenses $F1$ and $F2$ are assumed to be high enough so that overtopping and/or overflow of these defenses has no contribution to the bay inflow.
- The surge levels inside and outside the bay are transformed into annual water level exceedance probabilities by means of crude Monte Carlo simulations using $5 \cdot 10^4$ samples. These extreme water level distributions are used as the 'Load' part of the reliability equation Z in Eq. 14.

The 'Strength' part of the reliability equation Z (Eq. 14) is chosen to be a lognormal distribution, where the height of the flood defense functions as the mean, with a Coefficient of Variation (COV) estimated at twenty percent. The height of the defense is assumed to be equal to the critical water level (at which the defense breaks). The choice for the lognormal distribution is of a practical nature, because it produces strictly positive real values. Using a strength distribution based on the height of a flood defense, instead of a deterministic height, represents that additional failure mechanisms can occur besides overflow/overtopping. For example, piping can lead to failure for surge levels below the crest level (e.g. see [22]).

5.1.2. Estimation of failure probabilities

The raw Monte Carlo results of the surge simulations in Section 5.1.1 are approximated with generalized Pareto distributions (GP, threshold parameter fixed at 0) using maximum likelihood estimation in Matlab. Using probability distributions allows a straightforward application of, for example, a First Order Reliability Method (FORM) or a numerical integration routine. An overview of the used heights, flood damages, and load distributions can be found in Table 1.

Finally, because the loads and strength are now defined, each (conditional) failure probability of Eqs. 17 - 20 can be found. This involves solving the reliability equation Z (Eq. 14) where $Z < 0$, and is done using numerical integration. Assuming independence between the load S and strength R, the reliability equation where $Z < 0$ can be rewritten into a failure probability $P(Z < 0)$ as is done in, for example, [31]:

$$P(Z < 0) = \int_{-\infty}^{\infty} F_R(h)\, f_S(h)\, dh \quad (21)$$

where $F_R(h)$ is the cumulative distribution function of the resistance, and $f_S(h)$ is the probability density function of the load. The computed (conditional) failure probabilities will be used in Eq. 17 to calculate annual system risks.

5.2. Investment costs

The investment costs will be crude estimates based on [25] and [15]. In the case of [25], single value estimates are given for constructing defenses, while in [15] unit costs (per kilometer) are given. Without making an actual design, it will be difficult to obtain accurate investment costs, especially in the form of Eq. 15 where estimates of both fixed and variable costs are required. Therefore, the investment costs (Table 2) are loosely based on numbers found in [15] & [25], using an exponential investment relation (Eq. 15). The exponential scale parameter λ

Table 1: Reference level ($h_{i,ref}$, relative to MSL), height (h_i, relative to $h_{i,ref}$), potential flood damage (D_i) and annual Generalized Pareto (GP) water level distribution parameters for all the flood defenses.

Defense i	$h_{i,ref}$ $[m]$	h_i $[m]$	D_i $[10^9\$]$	$P_{i\|\overline{B1}}(\xi,\ \sigma)$	$P_{i\|B1}(\xi,\ \sigma)$
$B1$	0.0	0.0 - 20.0	0.0	-0.30, 2.2	-0.30, 2.2
$F2$	2.0	3.0	2.4	-0.30, 2.2	-0.30, 2.2
$F3$	2.0	3.0	4.8	-0.14, 0.56	-0.082, 0.89
$A1$	2.0	0.0 - 20.0	see $F2$	-0.14, 0.56	-0.082, 0.89
$A2$	2.0	0.0 - 20.0	38.5	-0.15, 0.77	-0.14, 1.3

Table 2: Investment costs for the to-be optimized flood defenses.

Defense i	$C_{f,i}$ [\$]	$C_{v,i}$ [\$/m]	Comments
$B1$	$3 \cdot 10^9$	$1 \cdot 10^9$	Storm surge barrier: Based on an estimated cost range of four to ten billions dollars [25].
$A1$	$300 \cdot 10^6$	$150 \cdot 10^6$	Levee: Estimated at ten million dollar per kilometer length, per meter defense heightening, which is on the high end of the range for the United States according to [15]. The length is estimated at 15 kilometers.
$A2$	$1 \cdot 10^9$	$300 \cdot 10^6$	Levee: Uses the same base estimate as defense $A1$. An additional 400 million dollars is added to the fixed costs to account for a gate solution at the north side of the bay [25]. The length is estimated at 30 kilometers.

for the investment relation of Eq. 15 is estimated at 0.02/m. An exponential relation is chosen because it allows to incorporate the assumed notion that costs increase exponentially for higher flood defenses. For example, with λ set at 0.02, an increase of defense $B1$ from zero to five meters would result in 8 billion dollars and 8.8 billion dollars for a linear and an exponential relation, respectively.

5.3. Economic optimization and time dependent parameters

As mentioned in Section 4.3, the economic optimization model uses the same model as used in [37]. For all flood defenses, a potential height range between zero and twenty meters was evaluated, with steps of one meter. The evaluated time period is 300 years, with steps of one year for the first twenty years, steps of five years between 20 and 100 years, and steps of ten years between 100 and 300 years. This time discretization is based on [38]. Because the time periods have a variable length, the risk for a period is calculated by finding the integral over that period for the (discounted and adjusted for economic growth) risk. Furthermore, a minimum timespan between investments of five and ten years was imposed for consecutively the rear and front defenses.

The time dependent parameters economic growth, interest rate and sea level rise are assumed to be constant in time for all flood defenses. First, the economic growth is estimated at six percent, which is at the low end of the average economic growth in a recent period of twelve years according to [28]. Secondly, the real interest rate in recent years varied between zero and four percent [29], and is estimated at two percent. Lastly, the sea level rise is determined using [21], and is estimated at 6.9 millimeters per year.

5.4. Results

Both the simplified method of Section 3 and the numerical framework of Section 4 are applied to the case study using the gathered input of the previous sections. The results are used to assess the load reduction effect of a front defense in this case study.

5.4.1. Load reduction effect: simplified method

Before the simplified method of Section 3 can be applied, a number of simplifications need to be made: the rear defenses $A1$ and $A2$ are summed into a single flood defense which uses the water level distribution of $A1$, flood defenses $F1$, $F2$ and $F3$ are ignored, economic growth and sea level rise are ignored, and the reliability of each flood defense is converted into an exponential function as used in Section 3.3. The results of these simplifications can be found in Table 3 and Figure 9.

The exponential functions in Figure 9 had to be manually fitted in order to get a reasonable approximation of the results found in Section 5.1.1. This figure shows that for annual exceedance probabilities larger than approximately $5 \cdot 10^{-2}$, the exponential fit significantly overestimates the associated water levels. However, the simplified method is meant to give insight into the behavior of the load reduction effect in a coastal system and not an accurate answer of the economically optimal safety targets. For the purpose of the simplified method, the exponential fits are considered acceptable.

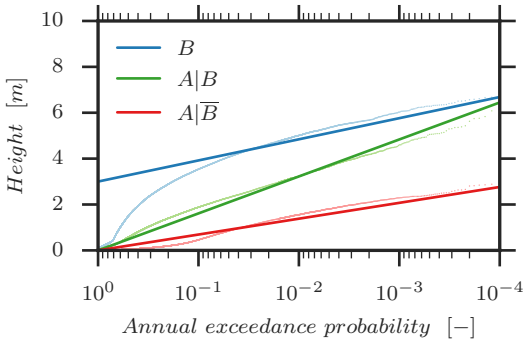

Figure 9: Exponential annual water level exceedance probabilities (solid lines, see also Table 3) which are used for the front defense B (line B) and the rear defense A (line $A|B$ if the front defense failed, otherwise line $A|\overline{B}$). The dotted lines are the Monte Carlo results.

Table 3: Input values for the application of the simplified economic optimization in the Galveston Bay area.

Parameter	Value	Unit
$\alpha_{A\|B}$	0.0	m
$\beta_{A\|B}$	0.7	m
$\alpha_{A\|\overline{B}}$	0.0	m
$\beta_{A\|\overline{B}}$	0.3	m
α_B	3.0	m
β_B	0.4	m
$C_{v,A}$	$450 \cdot 10^6$	$\$/m$
$C_{v,B}$	$1.0 \cdot 10^9$	$\$/m$
D_A	$40.9 \cdot 10^9$	\$
D_B	0.0	\$
r	0.02	–

The results of the simplified economic optimization are shown in Figure 10. First of all, the graph in this figure indicates that there is no difference regarding the optimal safety targets with or without a load reduction. Secondly, not building a front defense ($\widehat{P}_B = 1$) should be economically optimal. And thirdly, although arguably less relevant given the manually fitted exponential distributions, the economically optimal failure probability of the rear defenses should be in the order of $2 \cdot 10^{-4}$, which coincides with a levee height of approximately six meter.

The added value of the simplified model is that it can explain why there is no difference between including the load reduction and not including the load reduction. First of all, because the flood damage associated with a failed front defense (D_B) is set to zero, the logical consequence is that, if a load reduction is not included, not building a front defense is the economically optimal choice (see also Eq. 10). When the load reduction is included, Eq. 10 changes into Eq. 9, where only the denominator is different. In order for a front defense to be economically efficient and thus have a failure probability smaller than one, the denominator should be larger than the numerator:

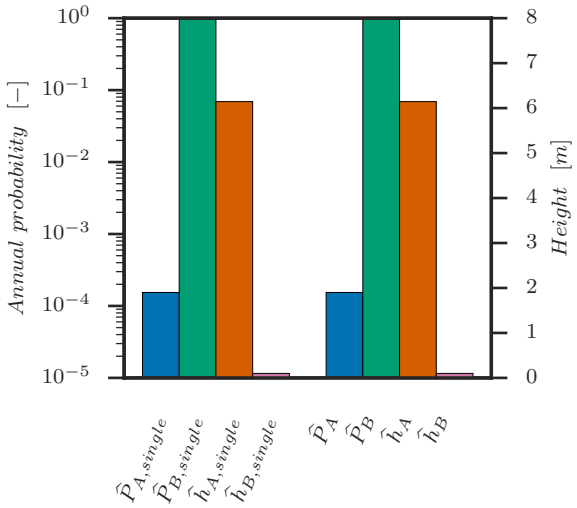

Figure 10: Result of the simplified economic optimization for the Galveston Bay area, using the input values of Table 3.

$$D_A \left(\widehat{P}_{A|B} - \widehat{P}_{A|\overline{B}} \right) > \beta_B C_{v,B} r \tag{22}$$

If Eq. 22 is used with the input of Table 3, together with a height of six meters for the rear defense, the result is $7.75 \cdot 10^6 > 8.00 \cdot 10^6$. This means that the risk reduction for the rear defense by the front defense (left hand side of Eq. 22) is not efficient when compared to the required investment of the front defense (right hand side of Eq. 22). However, the difference between the two numbers is relatively small, which means that if any of the relevant parameters change, a front defense might become an economically efficient choice after all. These parameters can change for example by including economic growth, sea level rise, or better approximations of the reliability of the defenses. In order to assess the effect of these potential changes, a numerical economic optimization is needed.

5.4.2. Load reduction effect: numerical method

In contrast to the application of the simplified method, the numerical framework is not limited to exponential water level distributions and can therefore use the better fitting generalized Pareto distributions of Table 1. The used water level distributions are shown in Figure 11 & 12.

The numerical framework was applied to the case study with and without the load reduction effect of the $B1$ front defense. Because the flood damage associated with a front defense failure (D_B) is set to zero, this implies that when the load reduction effect is not included, a front defense will never be economically optimal. The results of applying the numerical framework described in Section 4, using the input of Sections 5.1 - 5.3, are shown in Table 4 and Figure 13 (with load reduction) and in Table 5 and Figure 14 (without load reduction).

The load reduction effect can be observed when comparing the results of the numerical economic optimization in Table 4 and Figure 13. The rear defenses, after their initial upgrade in year 0, do not get upgraded until year 150. However, because

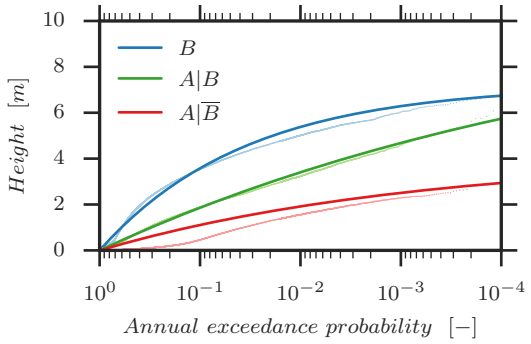

Figure 11: Annual water level exceedance probabilities which are used for flood defenses $B1$ & $F2$ (line B), and $A1$ & $F3$ (line $A|B$ if the front defense failed, otherwise line $A|\overline{B}$). The Generalized Pareto distributions (solid lines) are fitted to the Monte Carlo results (dotted lines).

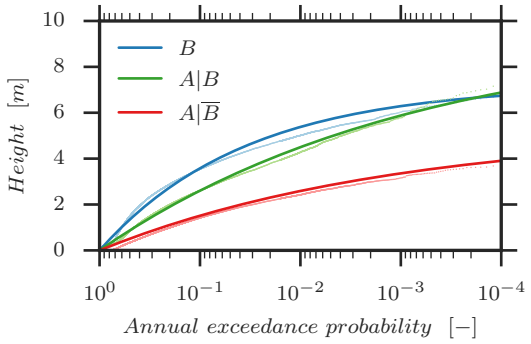

Figure 12: Annual water level exceedance probabilities which are used for flood defenses $B1$ & $F2$ (line B), and $A2$ (line $A|B$ if the front defense failed, otherwise line $A|\overline{B}$). The Generalized Pareto distributions (solid lines) are fitted to the Monte Carlo results (dotted lines).

of the load reduction effect of the front defense, upgrading the front defense $B1$ at $T = 30$ and $T = 100$ decreases the failure probabilities of the rear defenses as well. Additionally, the optimal heights of the rear defenses with the load reduction effect in Table 4 are also lower than the optimal heights without a load reduction effect in Table 5. Not only does the optimal system configuration change significantly from Table 5 to Table 4, the total cost estimate changes as well. For the first 50 years, the total cost decreases from $245.5 \cdot 10^9$ for the optimal investment scheme of Table 5 to $\$220.3 \cdot 10^9$ for the optimal investment scheme of Table 4.

The insight of the simplified method can be used to further explain some of these findings provided by the numerical method. First of all, the height reduction of the rear defenses when a load reduction is taken into account was already predicted in Section 3.4, and can be observed in Table 4 & 5. Secondly, Section 5.4.1 predicted that building no front defense was economically optimal, however the distance to the tipping point (where a front defense is economically viable) was found to be relatively small. This meant that the point where a front defense becomes economically viable could be reached in time when the time dependent parameters of Section 5.3 are included. The numerical framework predicts in Table 4 that this tipping point is reached after thirty years.

Finally, the optimal values of the simplified method for the rear defense in Figure 10 match the optimal values of the numerical framework for the first thirty years in Table 4 and Figure 13, despite the simplifications and exponential distributions used in the simplified method. This can possibly be explained by the fact that the exponential distributions fit reasonably well in the region of the found optimal failure probability ($\approx 10^{-4}$). Nevertheless, this does not change the fact that the simplified method of Section 3 still has too many simplifications for accurately quantifying economically optimal targets in practice; the simplified method should only be used to gain additional insight in parallel to a numerical economic optimization as described in Section 4.

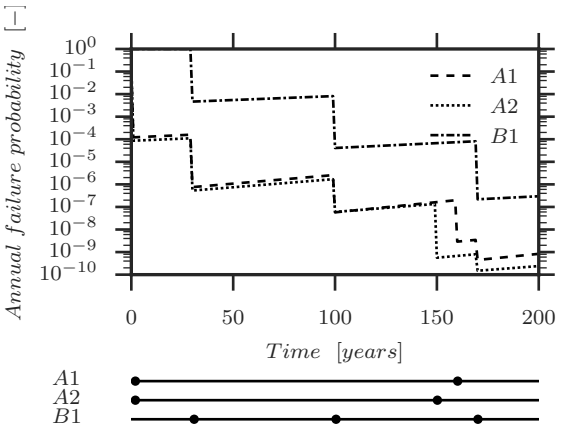

Figure 13: Safety values in time for flood defenses $B1$, $A1$ and $A2$ of Table 4, *with* the influence of a front defense. The corresponding timing of the investments per defense is shown as well.

Table 4: Optimal investment scheme for the Galveston Bay example using the numerical framework of Section 4, *with* the influence of a front defense.

Year	Defense	Height increase
0	$A1$	from 0 to 5 meter
160	$A1$	from 5 to 7 meter
0	$A2$	from 0 to 7 meter
150	$A2$	from 7 to 10 meter
30	$B1$	from 0 to 7 meter
100	$B1$	from 7 to 11 meter
170	$B1$	from 11 to 15 meter

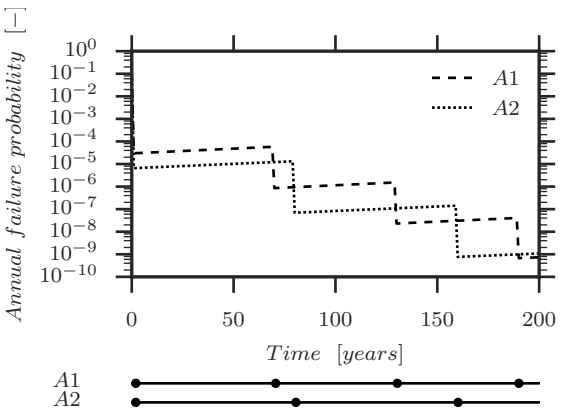

Figure 14: Safety values in time for flood defenses $A1$ and $A2$ of Table 5, *without* the influence a front defense. The corresponding timing of the investments per defense is shown as well.

Table 5: Optimal investment scheme for the Galveston Bay example using the numerical framework of Section 4, *without* the influence of a front defense.

Year	Defense	Height increase
0	$A1$	from 0 to 6 meter
70	$A1$	from 6 to 9 meter
130	$A1$	from 9 to 12 meter
190	$A1$	from 12 to 15 meter
0	$A2$	from 0 to 9 meter
80	$A2$	from 9 to 13 meter
160	$A2$	from 13 to 17 meter

6. Conclusions

The aim of this study was to develop a framework in order to assess whether including the influence of such a load reduction influences the economically optimal safety targets of a coastal flood defense system. This was done with the development of a simplified method, a flexible numerical framework and a case study.

The simplified method has a number of assumptions which make it not suitable for an actual quantification of the economically optimal safety targets, but it does provide additional insight into the influence of a load reduction on the economically optimal safety targets of a coastal flood defense system with a front and rear defense. This additional insight is provided in the form of analytical predictions regarding the expected effects of including a load reduction by a front defense. First of all, it showed that, in practice, the optimal height of rear defenses decreases when the load reduction effect is included. Secondly, the simplified method showed that the influence of a load reduction on the optimal safety target of a front defense is determined by the relative impact this front defense has on the flood risk of the rear defenses.

The answer of the simplified method does not account for a changing flood risk over time due to time dependent parameters such as economic growth or sea level rise. A changing flood risk over time opens up the possibility that even though a front defense is not the optimal choice right now, it might become economically optimal in the future. In order to be capable of providing practically applicable answers which include time dependency, a numerical framework is proposed.

The proposed numerical framework is capable of incorporating these time dependent parameters and can produce optimal safety targets over time. Furthermore, the numerical framework lifts a number of the restrictions set in the simplified method, therefore making it more practically applicable. It does this by integrating practically applicable hydraulic models, probabilistic methods and economic optimization methods.

Whether or not a load reduction has a significant effect on the economically optimal safety targets depends strongly on the particular characteristics of a flood defense system. To that end, a hypothetical case study (based on an actual case study) was contemplated in order to quantify the effects of a load reduction in this case study. This particular case study showed a significant effect by the load reduction on the economically optimal safety targets over time. Moreover, the load reduction effect significantly reduced the estimate of the total costs as well. Given the potentially large efficiency improvements regarding both the economically optimal safety targets and total cost estimate, not including the load reduction effect by a front defense on the economically optimal safety targets in coastal systems should be the exception to the rule.

Acknowledgements

We are grateful for the financial support of the Dutch Technology Foundation STW, which is part of the Netherlands Organization for Scientific Research, and which is partly funded by the Ministry of Economic Affairs.

References

[1] Aerts, J. C. J. H., Botzen, W., van der Veen, A., Krywkow, J., and Werners, S. (2008). Dealing with Uncertainty in Flood Management Through Diversification. *Ecology and Society*, 13(1).

[2] Bedient, P. and Blackburn, J. (2012). *Lessons from Hurricane Ike*. Texas A&M University Press.

[3] Brekelmans, R., Den Hertog, D., Roos, K., and Eijgenraam, C. (2012). Safe Dike Heights at Minimal Costs: The Nonhomogeneous Case. *Operations Research*, 60:1342–1355.

[4] CIRIA, CUR, and CETMEF (2006). *The Rock Manual. The use of rock in hydraulic engineering.* C683, CIRIS, London.

[5] Courage, W., Vrouwenvelder, T., van Mierlo, T., and Schweckendiek, T. (2013). System behaviour in flood risk calculations. *Georisk: Assessment and Management of Risk for Engineered Systems and Geohazards*, 7(2):62–76.

[6] Custer, R. (2015). *Hierarchical Modelling of Flood Risk for Engineering Decision Analysis.* Dissertation, Technical University of Denmark.

[7] De Bruijn, K. M., Diermanse, F. L. M., and Beckers, J. V. L. (2014). An advanced method for flood risk analysis in river deltas, applied to societal flood fatality risks in the Netherlands. *Natural Hazards and Earth System Sciences Discussions*, 2(2):1637–1670.

[8] Dupuits, E. and Schweckendiek, T. (2015). Flood risk and economically optimal safety targets for coastal flood defense systems. In Haukaas, T., editor, *ICASP12: 12th International Conference on Applications of Statistics and Probability in Civil Engineering, Vancouver, Canada, 12-15 July 2015*, Vancouver.

[9] Eijgenraam, C. (2005). Protection against flooding: Cost-benefit analysis for Space for the River, Part 1. Technical Report 82, The Hague.
[10] Eijgenraam, C. (2006). Optimal safety standards for dike-ring areas. Technical Report 62, CPB, The Hague.
[11] Faber, M. and Stewart, M. (2003). Risk assessment for civil engineering facilities: critical overview and discussion. *Reliability Engineering & System Safety*, 80(2):173–184.
[12] Faber, M. H., Sørensen, J. D., and Vrouwenvelder, A. C. W. M. T. (2015). On the regulation of life safety risk.
[13] Jongejan, R., Maaskant, B., ter Horst, W., Havinga, F., Roode, N., and Stefess, H. (2013). The VNK2-project: a fully probabilistic risk analysis for all major levee systems in the Netherlands. In *Floods: From Risk to Opportunity (IAHS Publ. 357)*, volume 2005, pages 75–85. IAHS Press.
[14] Jonkman, S., van Gelder, P., and Vrijling, J. (2003). An overview of quantitative risk measures for loss of life and economic damage. *Journal of Hazardous Materials*, 99(1):1–30.
[15] Jonkman, S. N., Hillen, M. M., Nicholls, R. J., Kanning, W., and van Ledden, M. (2013). Costs of Adapting Coastal Defences to Sea-Level Rise New Estimates and Their Implications. *Journal of Coastal Research*, 290:1212–1226.
[16] Kind, J. (2014). Economically efficient flood protection standards for the Netherlands. *Journal of Flood Risk Management*, 7(2):103–117.
[17] Kolen, B. (2013). *Certainty of uncertainty in evacuation for threat driven response. Principles of adaptive evacuation management for flood risk planning in the Netherlands*. Phd, Radboud Universiteit Nijmegen.
[18] Lendering, K. T., Jonkman, S. N., van Gelder, P., and Peters, D. J. (2015). Risk-based optimization of land reclamation. *Reliability Engineering & System Safety*, 144:193–203.
[19] Lickley, M. J., Lin, N., and Jacoby, H. D. (2014). Analysis of coastal protection under rising flood risk. *Climate Risk Management*, 6:18–26.
[20] Lund, J. R. (2002). Floodplain planning with risk-based optimization. *Journal of Water Resources Planning and Management*, 127(3):202–207.
[21] National Oceanic and Atmospheric Administration (2015). Tides and Currents. [Online; accessed 17-September-2015].
[22] Schweckendiek, T., Vrouwenvelder, A., and Calle, E. (2014). Updating piping reliability with field performance observations. *Structural Safety*, 47:13–23.
[23] Schweckendiek, T., Vrouwenvelder, A., Calle, E., Kanning, W., and Jongejan, R. (2013). Target Reliabilities and Partial Factors for Flood Defenses in the Netherlands. In Arnold, P., Fenton, G., Hicks, M., and Schweckendiek, T., editors, *Modern Geotechnical Codes of Practice - Code Development and Calibration*, pages 311–328. IOS Press.
[24] Small, C. and Nicholls, R. J. (2003). A Global Analysis of Human Settlement in Coastal Zones. *Journal of Coastal Research*, 19(3):584–599.
[25] SSPEED (2015). H-GAPS Houston-Galveston Area Protection System. Technical report, Rice University, Houston.
[26] Stoeten, K. (2013). *Hurricane Surge Risk Reduction For Galveston Bay*. M.sc. thesis.
[27] Tsimopoulou, V. (2015). *Economic optimisation of flood risk management projects*. Dissertation, Delft University of Technology.
[28] U.S. Department of Commerce (2015). Bureau of Economic Analysis. [Online; accessed 17-September-2015].
[29] U.S. Department of the Treasury (2015). Resource Center. [Online; accessed 17-September-2015].
[30] Van Dantzig, D. (1956). Economic Decision Problems for Flood Prevention. *Econometrica*, 24(3):276–287.
[31] van der Meer, J. W., ter Horst, W. L. A., and van Velzen, E. H. (2008). Calculation of fragility curves for flood defence assets. In *Flood Risk Management: Research and Practice*, pages 567–573. CRC Press.
[32] van der Pol, T., van Ierland, E., and Weikard, H.-P. (2014). Optimal dike investments under uncertainty and learning about increasing water levels. *Journal of Flood Risk Management*, 7(4):308–318.
[33] Voortman, H. (2003). *Risk-based design of large-scale flood defence systems*. Dissertation, Delft University of Technology.
[34] Vrijling, J. (2013). Multi layer safety. In *Safety, Reliability and Risk Analysis*, pages 37–43. CRC Press.
[35] Vrouwenvelder, A. (2014). Normstelling b-keringen. Private communication, TNO note.
[36] Zhu, T. and Lund, J. (2009). Up or out? - Economic-engineering theory of flood levee height and setback. *Journal of Water Resources Planning and Management*, 135(2):90–95.
[37] Zwaneveld, P. and Verweij, G. (2014a). Economisch optimale waterveiligheid in het IJsselmeergebied. Technical Report 10, CPB, The Hague.
[38] Zwaneveld, P. J. and Verweij, G. (2014b). Safe Dike Heights at Minimal Costs. Technical report, CPB, The Hague.